

The Effect of Pulse Charging on Commercial Lithium Cobalt Oxide (LCO) Battery Characteristics

D. Rajagopalan Kannan, M. H. Weatherspoon*

Department of Electrical and Computer Engineering, Florida A&M University - Florida State University College of Engineering, Tallahassee, Florida 32310, USA.

*E-mail: weathers@eng.famu.fsu.edu

Received: 23 August 2020 / Accepted: 18 October 2020 / Published: 28 February 2021

Lithium-ion batteries can be charged by different methods. CC-CV (constant current - constant voltage) charging is the conventional method that is predominantly employed for charging the batteries. Pulse charging is considered as an alternative charging method to reduce the charging time and increase energy efficiencies. However, the impact of pulse charging frequencies on the cycle life and battery behavior are seldom investigated. This paper presents the impact of pulse-CV charging at different frequencies (50 Hz, 100 Hz, 1 kHz) on commercial lithium cobalt oxide (LCO) cathode batteries in comparison to CC-CV charging. The results show that, on average, pulse-CV charging is considerably faster than CC-CV charging. It is also observed that pulse-CV charging at lower frequencies show comparable discharge capacities to CC-CV charging throughout cycling. Impedance characteristics of the battery were examined using electrochemical impedance spectroscopy (EIS) measurements and the impact of the charging methods has been analyzed based on the performance and electrochemical behavior of the batteries.

Keywords: Lithium cobalt oxide batteries; constant current – constant voltage; pulse-CV charging; charging time; cycle life; electrochemical impedance spectroscopy; equivalent circuit model

1. INTRODUCTION

Rechargeable lithium-ion batteries are widely used in many types of electronic devices because of their high energy density, broad operating temperature range, long cycle life and good electrochemical performance [1]. Research on lithium-ion batteries have produced high energy cathode materials which has helped in achieving high energy density for a similar sized lithium battery. The merits of the lithium-ion batteries have also made them as a promising power source for electric vehicles (EV's). Because batteries undergo charging and discharging processes regularly, fast charging, increased battery runtime and energy efficiencies are some of the important characteristics of

a lithium-ion battery. However, the process of fast charging causes degradation in the batteries which makes it unusable after a certain time period [2].

Lithium-ion batteries can be charged by different methods. CC-CV (constant current- constant voltage) charging is the conventional method that is predominantly employed for charging the batteries which is considered as a benchmark for comparisons [3]. Pulsed current charging is seen as one of the promising method for fast charging and high energy efficiencies [4–8]. However, the impact on the batteries due to the variations in the frequency of pulses have been seldom investigated on high energy density batteries.

Different charging methods have been proposed for reducing the amount of time to charge the batteries. Typical pulse charging procedures employ a strategy that provides periodical current pulses with short relaxation periods in-between to charge the battery. Researchers have proposed a variety of pulse charging procedures for recharging various types of battery chemistries with reduced charging time [5–9]. These procedures can be grouped into two categories (compared to CC-CV charging): pulse charging without the CV phase as in [5,7,8] and pulse charging with the CV phase as in [4,6]. The results from these studies provide contradictory conclusions on the pros and cons of pulse charging. The authors in [5,7,8] concluded that pulse charging results in (i) reduction of charging time, (ii) better utilization of active materials, and (iii) improvement of cycle life. However, from the findings in [4], it is concluded that pulse charging results in enhanced loss and poorer performance. Moreover, in [6], experiments of pulse-CV charging are performed at lower frequencies of 1 Hz and 25 Hz instead of higher pulse frequencies that are typically implemented in other studies.

The inconsistent conclusions in studies [4–8] can be attributed to two things: (i) differences in pulse frequency and (ii) inclusion/exclusion of the CV phase. In particular, inclusion of the CV phase results in increase of both charging time and charge capacity. Therefore, comparison of pulse charging (without the CV phase) with CC-CV charging will be an inappropriate comparison. Hence, in this work the impact of pulse-CV charging (including at different frequencies) on battery charging time, discharge capacity and impedance behavior are compared to CC-CV charging.

CC-CV charging of the lithium battery is done in two steps similar to the procedure in [5], and the two charging phases are constant current (CC) phase and constant voltage (CV) phase. During the CC charge phase, constant current is used until the battery reaches the maximum charge voltage. Then the CC charge phase transitions to the CV phase resulting in a decrease in charging current that prevents damage to the battery.

Typical charging time for the battery to reach full capacity can range from a half-hour to two hours in the CC phase and another half-hour to one hour in the CV phase. This varies depending on the charging current and maximum voltage rating of the battery. Charging the battery to higher voltages or at high currents reduces the cycle life due to the buildup of film on the anode after the initial formation of solid electrolyte interphase (SEI) [10].

Pulse-CV charging is a proposed method for fast charging which consists of rectangular current pulses along with the CV phase. In [11], it is suggested that (i) an optimal pattern of current pulses enhances the lithium-ion concentration during charging which results in a reduction of charging time and (ii) the selection of pulse attributes such as amplitude, frequency, and duty cycle impact the cycle life and impedance characteristics.

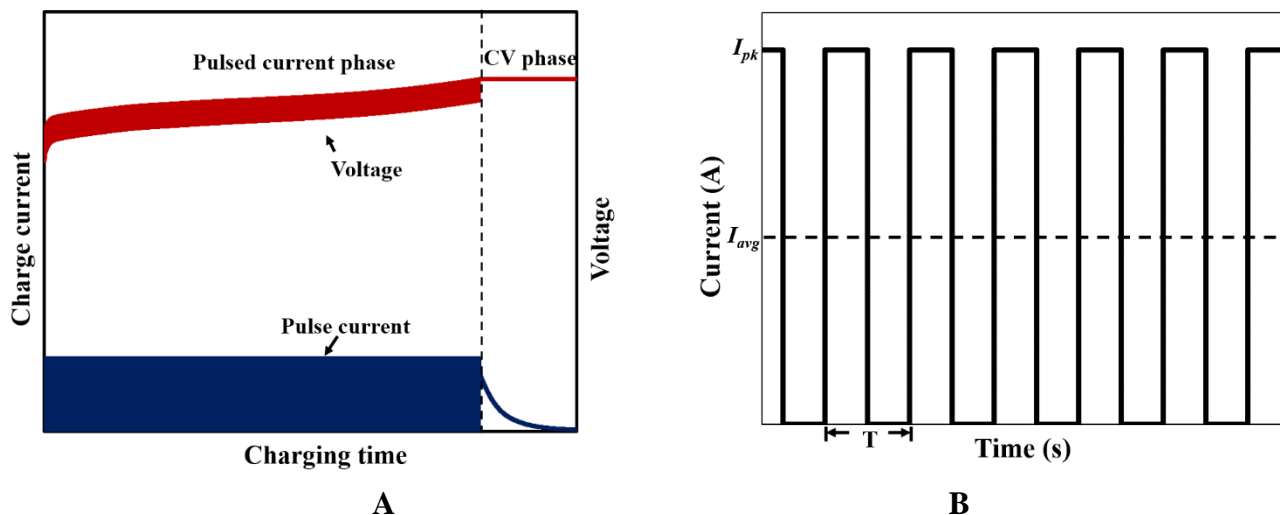


Figure 1. (a) Illustration of a pulse-CV profile for charging the lithium-ion battery, (b) Schematic representation of current pulse profile that is used in pulse charging where I_{pk} refers to peak pulse current, I_{avg} of the pulse is equal to constant current, and T refers to time period.

Figure 1(a) shows the voltage and current variation of the pulse-CV profile for a complete charging duration. Figure 1(b) shows the pulse profile where the peak current is denoted by I_{pk} , average current I_{avg} and time period T . The peak current and duty cycle values are chosen such that the average current is equal to the constant current used for testing. For a fixed duty cycle, the average current can be calculated using an equation in [5].

To determine the impact of pulse-CV charging on lithium-ion batteries, two different methods of evaluation are considered. The first method utilizes charging time and discharge capacity data to provide information on the electrochemical performance and capacity degradation in the batteries due to cycling. Side reactions and degradation processes in lithium-ion batteries may cause undesirable effects which result in capacity loss that negatively impacts performance. Typically, a lithium-ion battery is considered to have reached its end of life (EOL) when there is a 20% reduction from the initial capacity [12]. Therefore, in this study, the batteries were cycled until the capacity dropped to 20% of the initial rated capacity.

The second method utilizes electrochemical impedance spectroscopy (EIS) results to obtain relevant information on battery behavior. EIS is one of the most common non-destructive electrochemical methods that is used in analyzing batteries [2,13–21]. Typically, EIS measurements can be performed at any specific state of charge (SoC). However, the scope of EIS measurements in this study was limited to be performed at 100% SoC. An equivalent circuit model (ECM) can be created from the measured EIS data to obtain equivalent circuit parameters (ECPs) that correspond to various electrochemical processes within the battery [13,20]. This EIS data can include both positive reactance (inductive) and negative reactance (capacitive) parts depending on the frequency range of the measurement. And since it is known that the battery is inherently capacitive in nature, the inductive portion of the impedance is not necessary to accurately model the battery behavior. Hence in this work,

the EIS spectra are presented solely in terms of the capacitive portion of the EIS data, and the ECMs do not include inductors as part of their ECPs.

2. EXPERIMENTAL METHOD

A total of four commercially available LG 18650 batteries with LCO cathode were used for this study. Batteries were charged using CC-CV and pulse-CV methods at pulse frequencies of 50 Hz, 100 Hz, 1 kHz respectively. To remain consistent in the analysis, the average of pulse and conventional current were set to 1C while charging and discharging of the batteries. All the CC-CV and pulse-CV cycling of the batteries were performed using Neware BTS instruments. Table 1 shows the specifications of the battery that were used in this analysis.

According to the operating conditions in Table 1, the batteries were cycled between 0% - 100% SoC at room temperature using conventional and pulse-CV charging methods. CC and pulsed currents were used for charging during the initial phase until the batteries reached the maximum charge voltage and transitioned to the CV phase where the charge current decreased until it reached the cutoff current for both charging methods.

Table 1. Specifications of commercial LCO cathode lithium-ion batteries used in this study.

Battery Specifications	LCO
Nominal Voltage	3.6 V
Rated Capacity	2500 mAh
Charge Voltage	4.2 V
Cutoff Current	100 mA
Discharge Voltage	2.0 V

Based on the calculations for the LCO batteries, the pulse amplitude was set to 5000 mA at 50% duty cycle. The pulse width was calculated and set at 10 ms for 50 Hz, 5 ms for 100 Hz, and 0.5 ms for 1 kHz pulse. The versaSTAT4 instrument was used in galvanostatic mode to perform impedance measurements every 100 cycles at 100% SoC. The frequency for the EIS measurements was set from 20 kHz to 0.01 Hz, with 15 frequency points per decade. After the test, EIS results were exported to ZView for circuit modeling.

3. RESULTS AND DISCUSSION

To analyze the impact of different charging methods on the battery, the results with discussion are categorized and presented in sub-sections as follows: (i) battery performance characteristics, (ii)

impedance spectroscopy, (iii) equivalent circuit modeling. Following the experimental procedure described in Section 2, the batteries were cycled, and impedance measurements were performed.

3.1. Battery performance characteristics

Figure 2 (a) shows the comparison of charging time for different charging methods, and Figure 2 (b) shows the comparison of magnitude difference in charging times with respect to CC-CV. From the results, it clearly can be seen that the pulse-CV charging offers a significant decrease in charging time compared to CC-CV with the greatest time reduction occurring at the highest frequency of 1 kHz.

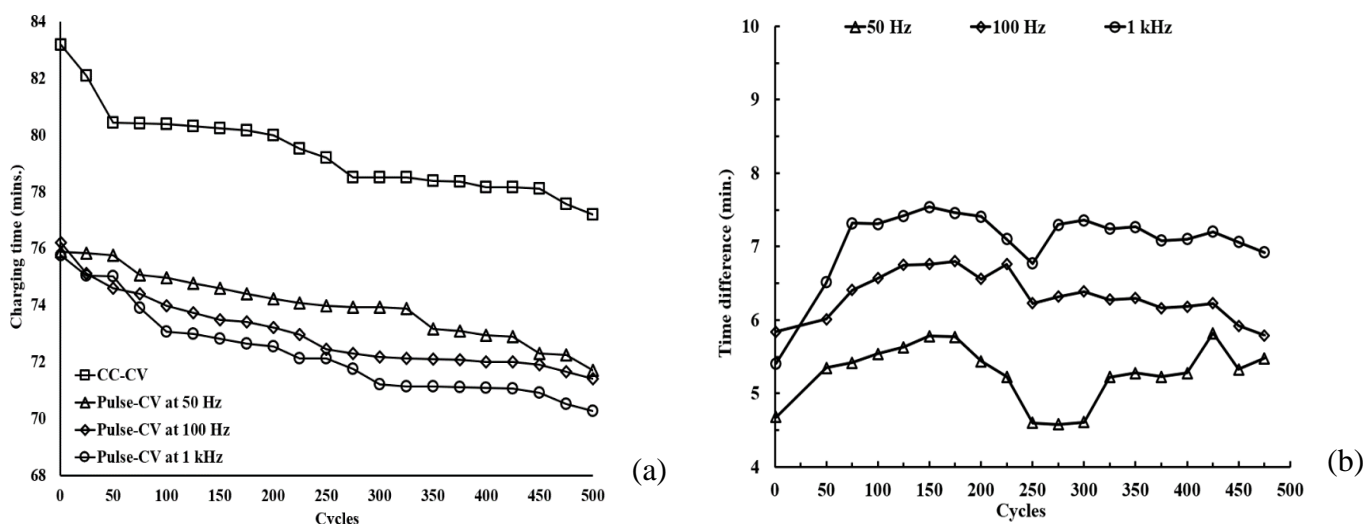


Figure 2. (a) Comparison of charging time vs. cycling for pulse-CV and CC-CV charging of LCO cathode lithium-ion batteries and (b) reduction in charging time at different pulse frequencies with respect to CC-CV.

Table 2. Percentage reduction in charging time for pulse-CV at different frequencies (with respect to CC-CV) vs. cycling of LCO cathode lithium-ion batteries.

Cycles	Pulse-CV at 50 Hz (%)	Pulse-CV at 100 Hz (%)	Pulse-CV at 1 kHz (%)
0	9.63	9.16	8.94
50	5.82	7.26	6.73
100	6.74	7.97	9.10
150	7.01	8.41	9.25
200	7.21	8.5	9.32
250	6.60	8.53	8.96
300	5.83	8.05	9.29
350	6.66	8.01	9.24
400	6.69	7.88	9.06
450	7.45	7.97	9.22
500	7.09	7.50	8.96
Max.	7.45	8.53	9.32
Min.	5.82	7.26	6.73
Avg.	6.71	8.01	8.91

Table 2 shows the percentage reduction in the pulse-CV charging time every 50 cycles with respect to CC-CV. On average 1 kHz pulse-CV charging is 8.91 % faster than CC-CV. Additionally, pulse-CV charging at 100 Hz and 50 Hz is 8.01 % and 6.71% faster respectively when compared to CC-CV.

The results in Figures 3 (a) and (b) show the discharge capacities of the different charging methods and the real difference in discharge capacities with respect to CC-CV for LCO batteries. The discharge capacities of CC-CV and pulse-CV at 50 Hz and 100 Hz are consistently better than pulse-CV charging at 1 kHz. Additionally, comparing the discharge capacities from 300 to 500 cycles shows that 50 Hz pulse-CV charging is slightly better than CC-CV.

Contained within Table 3 are the percentage differences in the pulse-CV charging capacities with respect to CC-CV at intervals of 50 cycles. The percentage reduction in capacity for 1 kHz pulse-CV charging is on average 2.96 which is approximately 22 times greater than the percentage reduction at 100 Hz. Furthermore, the much smaller average percentage changes at 50 Hz and 100 Hz when compared to 1kHz pulse-CV charging are indicative of better performance at the lower pulse frequencies over the cycle life of the battery.

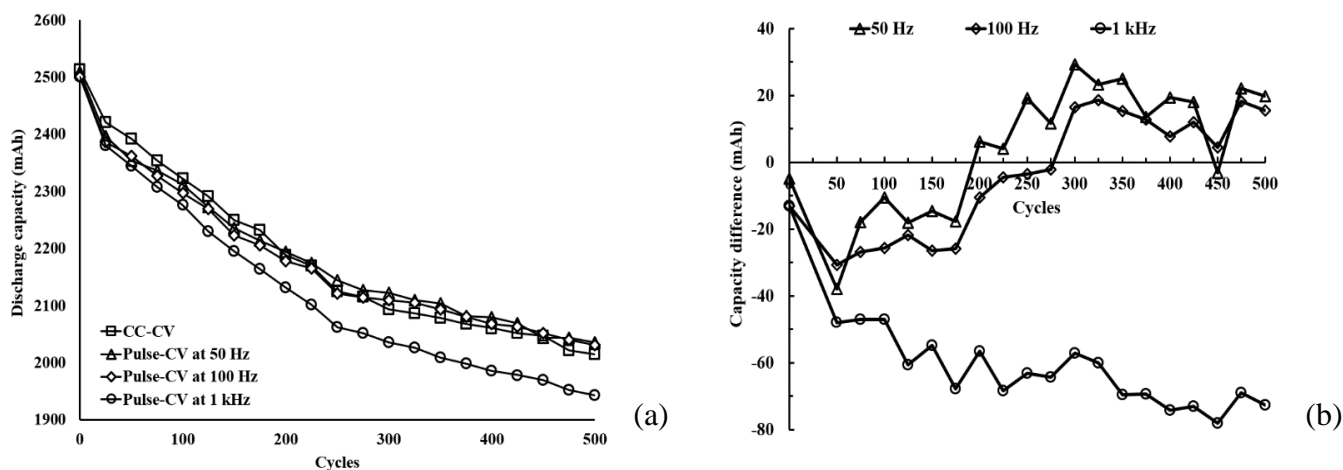


Figure 3. (a) Comparison of discharge capacity vs. cycling for pulse-CV and CC-CV charging of LCO cathode lithium-ion batteries and (b) change in discharge capacity with respect to CC-CV at different pulse frequencies.

As it can be observed in the results of this sub-section, pulse-CV charging is faster than CC-CV charging which is stated as one of the major benefits of using pulsed currents in the literature [5–9]. However, the papers which analyzed the pulse-CV charging [4,6] did not provide any data related to the charging time which makes the results of this work novel. It is also important to note in this work that the discharge capacity of pulse-CV charging at the lower frequency of 50 Hz has better average change in capacity when compared to CC-CV. On average, these results suggest that discharge capacity performance of the tested batteries is inversely proportional to pulse frequency.

Table 3. Percentage change in discharge capacity for pulse-CV at different frequencies (with respect to CC-CV) vs. cycling of LCO cathode lithium-ion batteries.

Cycles	Pulse-CV at 50 Hz (%)	Pulse-CV at 100 Hz (%)	Pulse-CV at 1 kHz (%)
0	-0.20	-0.52	-0.52
50	-1.58	-1.28	-2.03
100	-0.45	-1.11	-2.04
150	-0.65	-1.18	-2.47
200	0.28	-0.48	-2.61
250	0.90	-0.17	-3.02
300	1.40	0.78	-2.77
350	1.20	0.73	-3.40
400	0.94	0.37	-3.67
450	-0.15	0.21	-3.89
500	0.97	0.77	-3.67
Max.	1.40	0.78	-2.03
Min.	-1.58	-1.28	-3.89
Avg.	0.29	-0.136	-2.96

3.2. Impedance spectroscopy

Figure 4 shows the EIS plots for the LCO cathode lithium-ion batteries over cycling based on different charging methods. As described in section 1, only the negative reactance (capacitive) portion of the impedance spectra is presented. From the results, it can be observed that the impedance of the battery is clearly affected by different charging methods. For instance, Figure 4 (a) shows the impedance for CC-CV charging, and it can be observed that there is an increase in the ohmic resistance versus cycling. Moreover, there is only a slight increase in the initial EIS up to 300 cycles, whereas there is a significant increase in the ohmic resistance beyond 300 cycles. Additionally, from Figures 4 (b) and (c) it can be observed that, the increase in ohmic resistance for pulse-CV charging at 50 Hz and 100 Hz are similar to CC-CV charging. However, Figure 4(d) show that, for pulse-CV charging at 1 kHz the ohmic resistance increases considerably beyond 200 cycles and it is greater when compared to other types of charging.

Furthermore, from Figure 4(a) the impedance results for CC-CV charging show a similar reactance during the first 300 cycles beyond which there is a drastic increase. This type of increase is associated with cell degradation due to cycling [22]. Moreover, from the impedance results for pulse-CV charging as shown in Figure 4 (b) – (d), it can be observed that the reactance during the first 200 cycles increases gradually beyond which there is a significant increase. In addition, the reactance is substantially larger for all types of charging at the end of cycle life when compared with the initial 200 cycles.

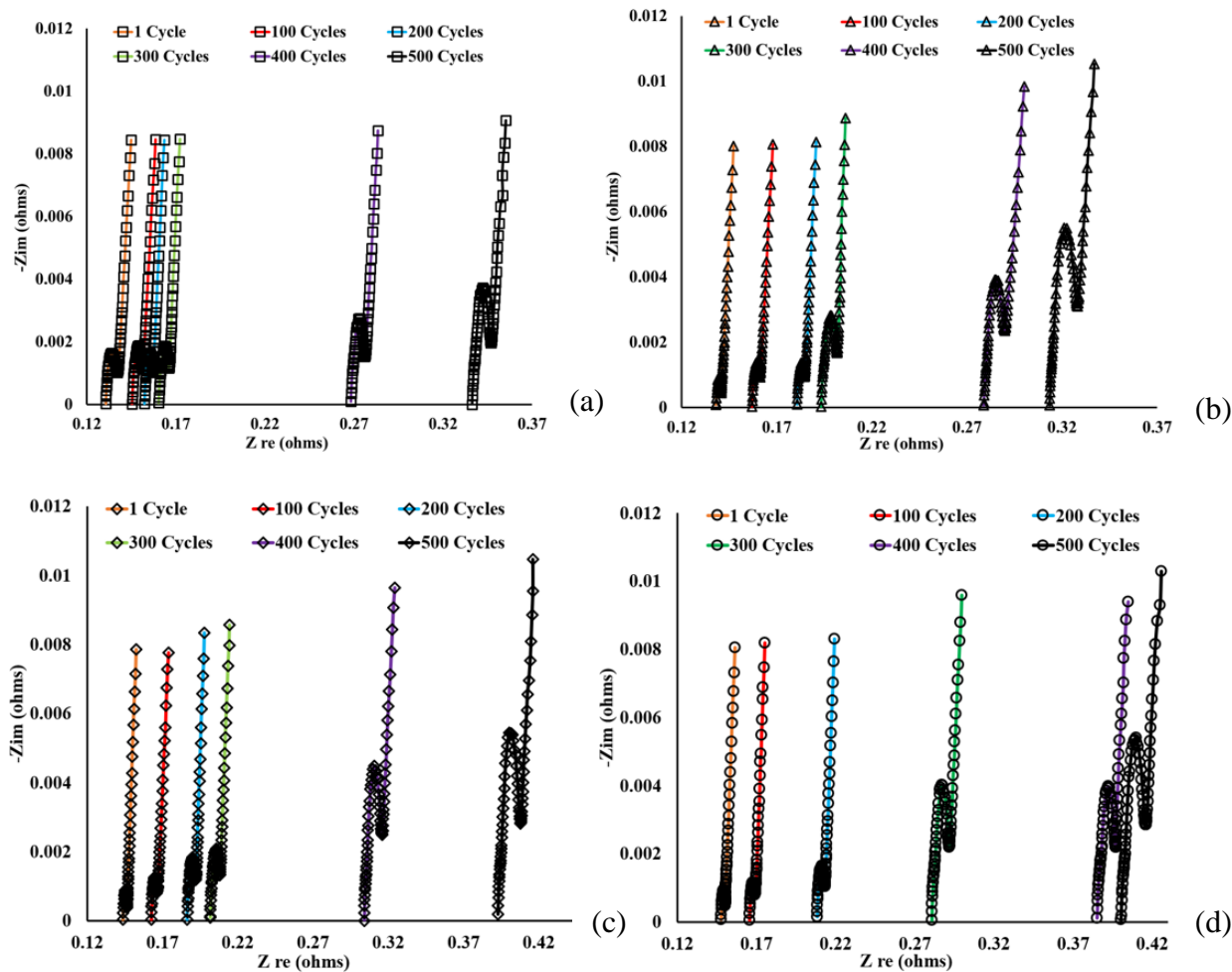
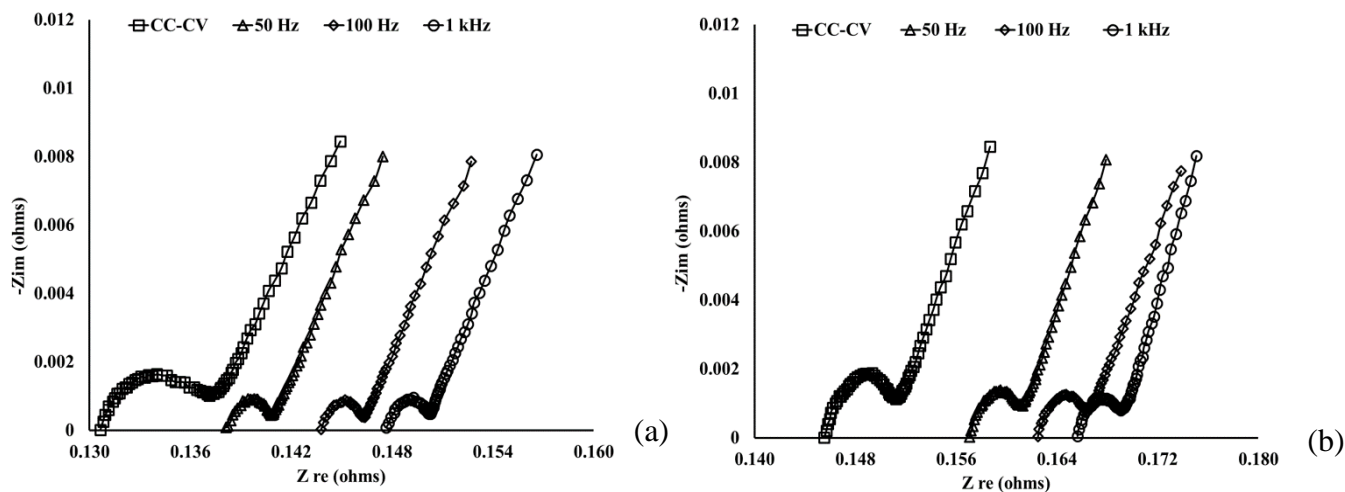


Figure 4. Capacitive impedance spectra of LCO cathode lithium-ion batteries based on different types of charging methods; (a) CC-CV, (b) pulse-CV at 50 Hz, (c) pulse-CV at 100 Hz and (d) pulse-CV at 1 kHz.



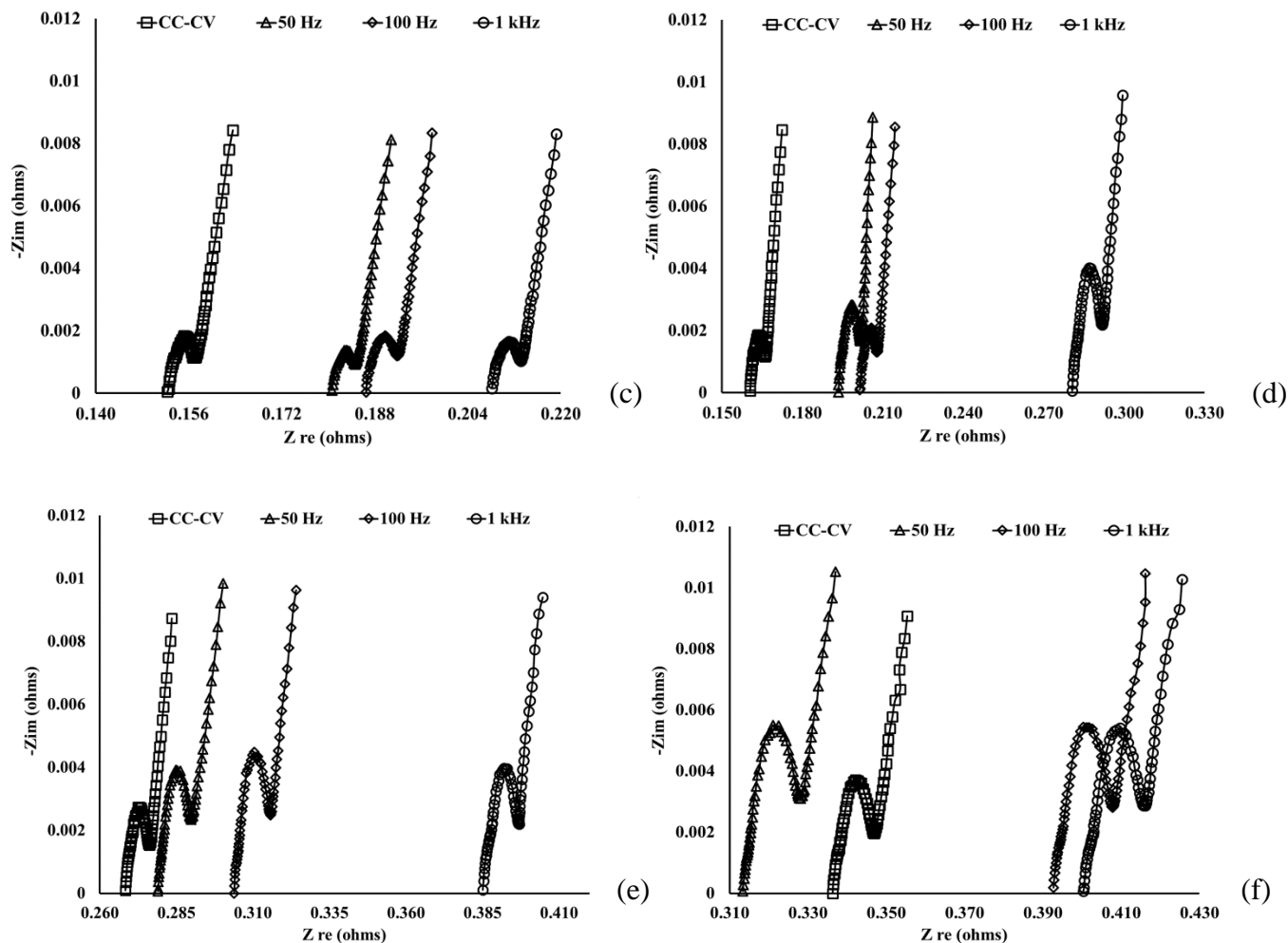


Figure 5. Capacitive impedance spectra of CC-CV and different pulse-CV charging procedures performed at 100% SoC; (a) 1 cycle, (b) 100 cycles, (c) 200 cycles, (d) 300 cycles, (e) 400 cycles and (f) 500 cycles.

Figure 5 (a) shows the preliminary EIS results after just one cycle. Figures 5(b)-(f) show the comparison of impedance spectra of different charging methods with respect to the number of cycles and are indicative of the true battery behavior. Over the first 300 cycles, in each of Figures 5 (b)-(d), it can be observed that the ohmic resistances increase versus frequency (with CC-CV considered to be at 0 Hz). For the next 200 cycles, in each of Figures 5 (e) and (f), it can be seen that there is a substantial growth in ohmic resistance when compared to the first 300 cycles. At 400 cycles, the ohmic resistances continue to increase versus frequency, but at 500 cycles this is no longer the case. More specifically, the 50 Hz pulse-CV shows a slightly lower ohmic resistance when compared to CC-CV.

The shape of Nyquist plots (Figures 4 and 5) obtained for different charging methods in this study are in accordance with similar Nyquist plots available in the literature [5,13,22–24], and the associated impedance of the Nyquist plots represents combined contributions from both electrodes and contains valuable information related to charge and mass transport [22]. Nyquist plots can be divided into three parts, namely mid-frequency, low-frequency, and high-frequency regions. The semicircle in

the mid-frequency region is typically associated with kinetic reactions, and depending on the utilization of the cell, additional semicircles can be observed in the high to mid-frequency region. The low-frequency slope line region represents the diffusion of Li-ion in the electrode. The high-frequency region (primarily observed in the positive reactance or inductive tail portion of Nyquist plots) is attributed to the porosity of the electrodes and jelly-roll structure of the cell [22,25,26].

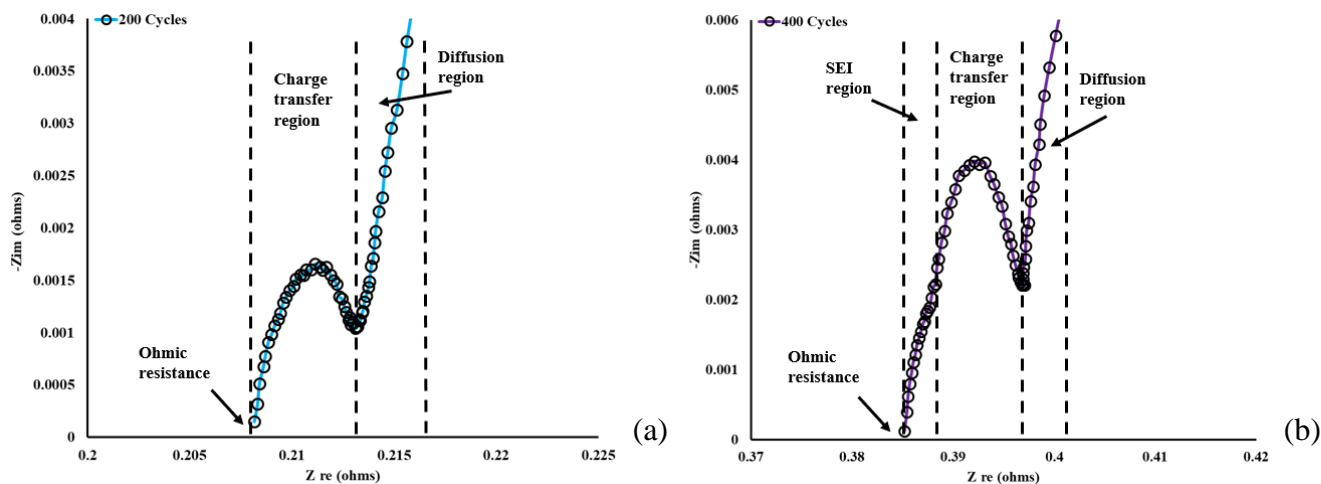


Figure 6. Partial portion of capacitive impedance spectra with individual mechanisms of 1 kHz pulse-CV charging at (a) 200 cycles and (b) 400 cycles to establish the difference in the high frequency portion.

Figures 6 (a) and (b) show a portion of the capacitive impedance spectra for 1 kHz pulse-CV charging at 200 and 400 cycles to establish the differences in the impedance spectra due to aging of the cell. Figure 6(a) shows that, for 200 cycles, there is one continuous semicircle which depicts the frequency domain of individual mechanisms occurring in the lithium-ion cell, whereas for 400 cycles (Figure 6(b)) there is an additional semicircle portion in the high to mid-frequency region that represents SEI layer formation.

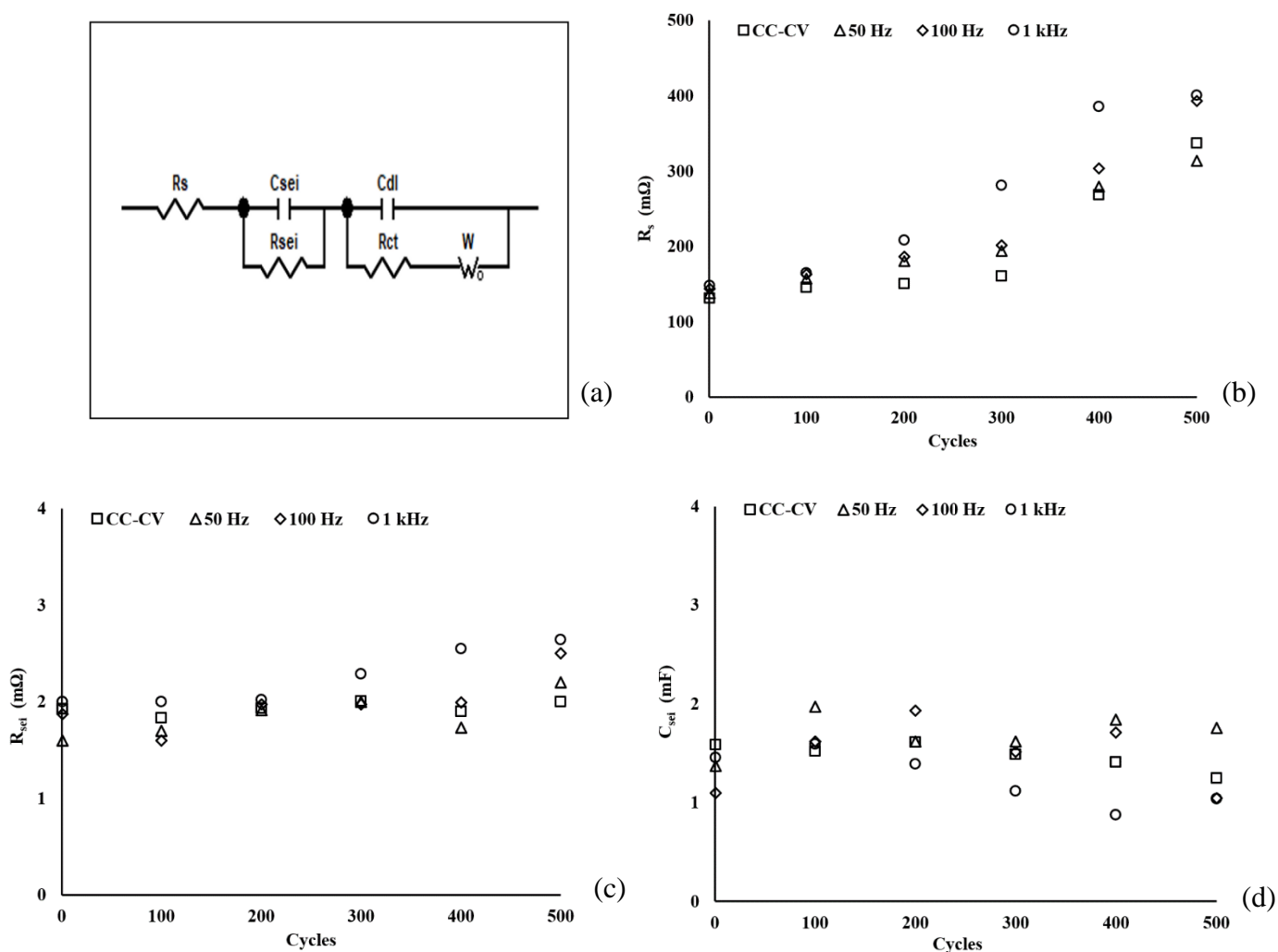
3.3. Equivalent circuit modeling

Figure 7 (a) shows the two-time constant equivalent circuit model that was used to fit the EIS spectra. In general, a single semicircle within a Nyquist plot can be characterized by a one-time constant ECM. However, based on the comparison of the EIS data presented in Figure 6, it is evident that the results contain a second semicircle. Therefore, a two-time constant ECM was chosen to fit the corresponding impedance spectrum and to obtain ECP values.

The application of these specialized ECP elements to describe electrochemical impedance behavior can relate the individual mechanisms to their impedance spectra. Specifically, the second semicircle present in the high to mid-frequency range is associated with the SEI layer that covers the

electrode and has equivalent resistance R_{sei} and corresponding capacitance C_{sei} [10,13,22,27]. The high frequency intercept of the real axis is associated with ohmic/solution resistance R_s which is correlated with ohmic polarization of the cell and can be ascribed to the electrolyte, separator, and contacts [22]. Lastly, the mid-frequency reactance is correlated with kinetic reactions which are characterized by charge transfer resistance R_{ct} and the associated double-layer capacitance C_{dl} [17,23].

Figures 7 (b) - (f) show the values of equivalent circuit parameters R_s (ohmic resistance), R_{sei} (resistance due to surface film), C_{sei} (capacitance due to surface film), R_{ct} (charge transfer resistance) and C_{dl} (double layer capacitance) versus cycling. Figure 7(b) shows the plot of R_s increasing versus cycling for different charging methods and is consistent with the results seen in Figure 5. The R_s for the battery pulse-CV charged at 1 kHz is consistently higher across all the cycles when compared to the battery charged with CC-CV. This suggests that higher pulse frequency might result in faster deterioration of battery cyclability [28]. Figure 7(c) shows comparable R_{sei} until 200 cycles for all charging methods with the 1 kHz pulse-CV charged battery having the larger value, and after 200 cycles there is a discernable increase in R_{sei} for 1 kHz pulse-CV charging which indicates larger growth in the interfacial layer. This growth occurs due to consumption of active lithium which results in increased capacity fade [10,22,29–31].



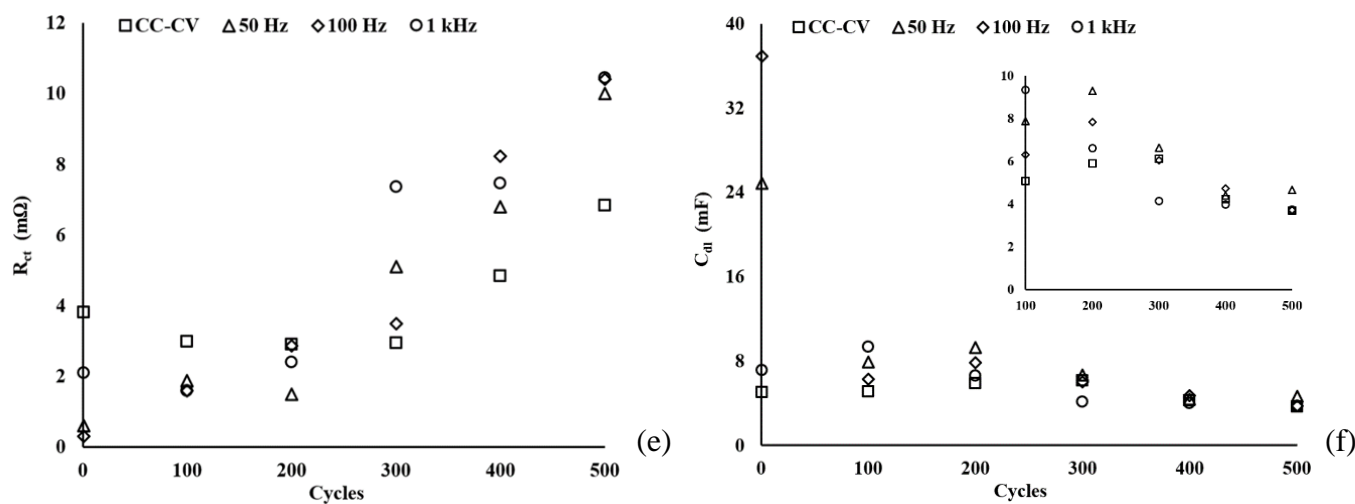


Figure 7. (a) Equivalent circuit model; (b)-(f) equivalent circuit parameters (R_s , R_{sei} , C_{sei} , R_{ct} and C_{dl} respectively) vs. cycling for CC-CV and pulse-CV charging of LCO cathode lithium-ion batteries (inset figure (f) shows C_{dl} starting from 100 cycles).

In contrast, R_{sei} for CC-CV charging is similar throughout the cycle life which indicates there is no significant growth in the interfacial layer. Figure 7 (d) shows the capacitance due to SEI with 1 kHz pulse-CV charging having the lowest values across the cycles when compared to other charging methods. The results under high frequency (1 kHz) pulse-CV charging procedure in Figure 7(c) suggest that there is a rapid increase in the formation of irreversible products after 200 cycles.

Figure 7(e) shows the variation in R_{ct} versus cycling, and for the first 200 cycles it is lower for the pulse-CV charging procedures than CC-CV charging. However, after 200 cycles there is an increasing trend in R_{ct} for the different charging methods with pulse-CV showing drastic increase when compared to CC-CV charging. This difference in R_{ct} suggests that pulse-CV charging might be better during the earlier cycles, but continuous cycling using pulsed currents might adversely impact the batteries. It is important to note that after 200 cycles the growth of R_{ct} for 50 Hz pulse-CV charging is lower when compared to 100 Hz and 1 kHz pulse-CV charging procedure. This is indicative of poorer performance of higher charging frequencies when compared to 50 Hz pulse-CV and CC-CV charging. Figure 7(f) shows the C_{dl} values versus cycling with slight variation in capacitance prior to 200 cycles and a general decreasing trend starting at 200 cycles for the different charging methods. The trends in Figures 7(e) and (f) starting at 200 cycles have an inverse relationship that are consistent with results reported for continuous cycling leading to increased R_{ct} and decreased C_{dl} due to poorer contact between the active materials and current collectors [21].

4. CONCLUSION

The influence of pulse-CV and CC-CV charging methods on the charging time, cycle life and impedance parameters on commercial LCO cathode lithium-ion batteries has been determined. Results

from the cycling of the batteries indicated that pulse-CV charging at 50 Hz, 100 Hz and 1 kHz at 50% duty cycle offers significant reduction in charging time when compared to CC-CV charging. In addition, pulse-CV charging at 50 Hz and 100 Hz showed comparable capacities to CC-CV charging whereas the battery that was cycled using 1 kHz pulse-CV charging showed a considerable reduction in capacity. The impedance measurements show that the behavior of the batteries is clearly impacted by different charging methods. There is a substantial increase in resistance and reactance beyond 200 cycles for different charging methods where the maximum increase was observed for 1 kHz pulse-CV charging. This indicates that pulse-CV charging at a higher frequency might be detrimental for LCO batteries. Though the pulse-CV charging at lower frequencies of 50 Hz and 100 Hz have larger reactance beyond 200 cycles when compared to CC-CV charging, reduction in charging time and comparable capacities throughout cycle life makes them more optimal for charging LCO cathode lithium-ion batteries.

References

1. J. Tan, A.M. Tartakovsky, K. Ferris, E.M. Ryan, *J. Electrochem. Soc.*, 163 (2016) A318–A327.
2. Y. Abe, N. Hori, S. Kumagai, *Energies*, 12 (2019) 1–14.
3. Y. Zhao, B. Lu, Y. Song, J. Zhang, *Front. Struct. Civ. Eng.*, 13 (2019) 294–302.
4. F. Savoye, P. Venet, M. Millet, J. Groot, *IEEE Trans. Ind. Electron.*, 59 (2012) 3481–3488.
5. J.M. Amanor-Boadu, A. Guiseppi-Elie, E. Sánchez-Sinencio, *Energies*, 11 (2018) 1–15.
6. P. Keil, A. Jossen, *J. Energy Storage*, 6 (2016) 125–141.
7. J. Li, E. Murphy, J. Winnick, P.A. Kohl, *J. Power Sources*, 102 (2001) 294–301.
8. C.-Y. Lin, S.-C. Yen, *ECS Trans.*, 11 (2008) 55–62.
9. F. Savoye, P. Venet, S. Pelissier, M. Millet, J. Groot, *IEEE Trans. Ind. Electron.*, 7 (2015) pp 323–341.
10. M.B. Pinsona, M.Z. Bazant, *J. Electrochem. Soc.*, 160 (2013) 1–29.
11. J.M. Amanor-Boadu, A. Guiseppi-Elie, E. Sánchez-Sinencio, *IEEE Trans. Ind. Electron.*, 65 (2018) 8982–8992.
12. S. Saxena, C. Le Floch, J. Macdonald, S. Moura, *J. Power Sources*, 282 (2015) 265–276.
13. M.E. Orazem, B. Tribollet, *Electrochim. Acta*, 53 (2008) 7360–7366.
14. P. Vyroubal, T. Kazda, *J. Energy Storage*, 15 (2018) 23–31.
15. B.T. Habte, F. Jiang, *Microporous Mesoporous Mater.*, 268 (2018) 69–76.
16. T. Hang, D. Mukoyama, H. Nara, N. Takami, T. Momma, T. Osaka, *J. Power Sources*, 222 (2013) 442–447.
17. T. Osaka, T. Momma, D. Mukoyama, H. Nara, *J. Power Sources*, 205 (2012) 483–486.
18. M.S. Wu, P.C.J. Chiang, J.C. Lin, *J. Electrochem. Soc.*, 152 (2005) 47–52.
19. B.S. Haran, A. Durairajan, P. Ramadass, R.E. White, B.N. Popov, *Proc. Intersoc. Energy Convers. Eng. Conf.*, 2 (2001) 935–940.
20. Salim Erol, *Electrochemical Impedance Spectroscopy Analysis and Modeling Of Lithium Cobalt Oxide/Carbon Batteries*, University of Florida, 2015.
21. V.J. Ovejas, A. Cuadras, *Batteries*, 4(3) (2018) 43.
22. P.L. Moss, G. Au, E.J. Plichta, J.P. Zheng, *J. Power Sources*, 189 (2009) 66–71.
23. A. Barai, G.H. Chouchelamane, Y. Guo, A. McGordon, P. Jennings, *J. Power Sources*, 280 (2015) 74–80.
24. J. Li, E. Murphy, J. Winnick, P.A. Kohl, *J. Power Sources*, 102 (2001) 302–309.
25. S. Rodrigues, N. Munichandraiah, A.K. Shukla, *J. Solid State Electrochem.*, 3 (1999) 397–405.

26. D. Zhou, Z. Liu, X. Lv, G. Zhou, J. Yin, *Electrochim. Acta*, 51 (2006) 5731–5737.
27. A. Barai, G.H. Chouchelamane, Y. Guo, A. McGordon, P. Jennings, *J. Power Sources*, 280 (2015) 74–80.
28. V. Yufit, P. Shearing, R.W. Hamilton, P.D. Lee, M. Wu, N.P. Brandon, *Electrochem. Commun.*, 13 (2011) 608–610.
29. M. Greenleaf, H. Li, J.P. Zheng, *J. Power Sources*, 270 (2014) 113–120.
30. Y.X. Lin, Z. Liu, K. Leung, L.Q. Chen, P. Lu, Y. Qi, *J. Power Sources*, 309 (2016) 221–230.
31. S.J. An, J. Li, C. Daniel, D. Mohanty, S. Nagpure, D.L. Wood, *Carbon N. Y.*, 105 (2016) 52–76.

© 2021 The Authors. Published by ESG (www.electrochemsci.org). This article is an open access article distributed under the terms and conditions of the Creative Commons Attribution license (<http://creativecommons.org/licenses/by/4.0/>).